Vibrational Deactivation of Highly Excited Hexafluorobenzene

Jason R. Gascooke,[†] Zeyad T. Alwahabi,[‡] Keith D. King,*[,‡] and Warren D. Lawrance[†]

Department of Chemistry, Flinders University, G.P.O. Box 2100, Adelaide SA 5001 Australia, and Department of Chemical Engineering, University of Adelaide, SA 5005, Australia

Received: March 25, 1998; In Final Form: June 4, 1998

Highly excited hexafluorobenzene (HFB) molecules in the electronic ground state were prepared by infrared multiphoton absorption by CO_2 laser pumping using the P(38) line at 1029.43 cm^{-1}. The vibrational deactivation of the highly excited HFB by monatomic collider gases was monitored by time-resolved infrared fluorescence (IRF). Deactivation measurements were made for the noble gas colliders He, Ne, Ar, Kr, and Xe. The bulk average energy transferred per collision, $\langle\langle \Delta E \rangle\rangle$, for these colliders was found to increase from He through to Ar; however it subsequently decreased from Ar through to Xe. This is different than the trend found in the quasiclassical trajectory calculations by Lenzer et al., which predict a decrease in the average energy transferred per collision from He to Ar to Xe. (Calculations were not reported for Ne and Kr.) However, similar trends in related energy-transfer parameters have been reported for the deactivation of C_6F_{14} and C_8F_{18} by the same series of five noble gases. A comparison is made with previous experimental measurements for the colliders He and Ar which were obtained using UV excitation of the HFB. For the same monatomic colliders, the $\langle\langle \Delta E \rangle\rangle$ values for HFB are much greater than those for the closely related aromatics, benzene, toluene, and pyrazine.

Introduction

Collision-induced energy transfer between molecules containing significant amounts of vibrational energy is an essential excitation and deexcitation mechanism in many gas-phase reactions.[1] Despite its importance, there is a paucity of knowledge concerning collisional deactivation from highly excited molecules, and many important questions await definitive answers. Two key questions are (i) what is the form of the collision energy step size distribution function $P(E',E)$ and (ii) what is the dependence of average energy transferred per collision on the internal energy of the excited molecule? For example, the energy dependence has been shown to be constant,[1] linear,[1] linear but rolling off at higher energies,[2] and linear above a certain threshold energy.[3] In the present paper we report the results of experiments that provide insights into the second of these questions.

Direct measurements of collisional energy transfer from highly excited molecules have usually relied on UV pumping of a molecule to an excited electronic state, followed by nonradiative intramolecular transfer to high-lying vibrational levels in the ground electronic state as the means of state preparation.[1,2] Producing an ensemble of excited molecules through rapid internal conversion has the advantage that the initial energy distribution is extremely narrow and defined, centered about the excitation wavelength of the light source used. Infrared multiphoton absorption (IRMPA) provides an alternative method for initial preparation of large populations of highly excited molecules in the ground electronic state with various initial internal energies.[4−7] An ensemble of excited molecules are produced which become vibrationally equilibrated during and shortly after the IR pulse. The average internal energy the excited molecule initially reaches after IRMPA is controlled by varying the fluence of the excitation laser. The disadvantage in using IRMPA is the uncertainty in the initial energy distribution.[4,5] Nevertheless, the average excitation energy is readily determined, and it has been shown that under appropriate conditions the results extracted from the data depend solely on this; i.e., they are independent of the initial distribution.[8,9] In a recent direct comparison of the UV and IRMPA methods of excitation in collisional energy-transfer studies, we have shown that for the same molecule and collider gas pair the two methods produce identical results within experimental error.[10]

In the direct studies of large molecule collisional energy transfer, time-resolved monitoring of the energy content of the highly vibrationally excited molecules has been carried out using IRF or hot-band UV absorption spectroscopy.[1] IRF has generally been used with cyclic ring systems, usually aromatics, excited by internal conversion (IC) following visible/UV excitation (hereafter referred to as IC-IRF), as has UV absorption spectroscopy (hereafter referred to as IC-UVA). There have been very few studies using the combination of IRMPA coupled with time-resolved IRF (hereafter referred to as IRMPA-IRF).[5,7,11]

HFB has excellent attributes for energy-transfer studies. It is a large molecule that undergoes rapid IC after UV excitation with near unit quantum efficiency.[12−14] This allows initial-state preparation using an excimer laser at either 193 or 248 nm. HFB is very stable, requiring >1700 K to initiate any thermal decomposition[13] and >60 000 cm^{-1} for photochemical decomposition.[15] Because of these photophysical properties, collisional deactivation of highly excited HFB has previously been the subject of experimental[12,13] and complementary theoretical studies.[16,17] Previous workers have used the IC-UVA technique with excitation at 193 nm.[12,13] Ichimura et al.[12] carried out measurements for the colliders Ar, N_2, O_2, and HFB, while

[†] Flinders University.
[‡] University of Adelaide.

10.1021/jp981620d CCC: $15.00
Published on Web 07/17/1998

Damm et al.[13] investigated the colliders He, Ar, N_2, O_2, C_3H_8, n-C_8H_{18}, and n-C_8F_{18}.

HFB has two very strong IR absorption bands at 1007 and 1530 cm^{-1},[18] the former being coincident with CO_2 laser output, thus making it a suitable candidate for IRMPA-IRF studies and allowing direct comparison between the IRMPA-IRF and IC-IRF techniques.[10] In the present study, we used the technique of IRMPA-IRF with CO_2 laser pumping at 1029.43 cm^{-1} and time-resolved IRF of the band at 1530 cm^{-1}. Experimental results were obtained for the monatomics He, Ne, Ar, Kr, and Xe as collision partners. The analysis of the IRF decays leads to insights into the variation of the bulk average energy transferred per collision, $\langle\langle \Delta E \rangle\rangle$, with internal energy of the HFB molecules. To obtain insights into this behavior at higher internal energies, we have undertaken limited studies using IC-IRF with excimer laser pumping of HFB at 248 nm.[10] Our results are compared with previous experimental work[12,13] and with recent quasiclassical trajectory calculations on the deactivation of highly excited HFB by He, Ar, and Xe.[16,17]

Experimental Section

The experimental system for the IRMPA-IRF experiments is a more elaborate version of the experimental design used for recent studies of the collisional deactivation of vibrationally excited CO_2 and N_2O.[19] A full description of the experimental system is given elsewhere.[10] Briefly, infrared laser radiation from a pulsed CO_2 laser (Lumonics TEA 103-2) tuned to the P(38) laser line at 1029.43 cm^{-1} is directed through a Galilean telescope and then into a cylindrical fluorescence cell constructed from stainless steel and fitted with NaCl end windows. The IRF from the excited HFB molecules was monitored perpendicular to the laser beam axis through a MgF_2 side window and a band-pass filter centered at 1486 cm^{-1} (bandwidth 167 cm^{-1}) with a liquid nitrogen cooled HgCdTe detector (Infrared Associates) equipped with a matched preamplifier (combined rise time ~400 ns). The detector/preamplifier output was captured by a digital storage oscilloscope (LeCroy 9310) and transferred to a laboratory computer for analysis. The oscilloscope was used to average decay curves for ~200 pulses at a laser pulse repetition frequency of ~1 Hz, to achieve adequate signal-to-noise ratios.

Extreme care was taken in the measurements of the average number of IR photons absorbed per HFB molecule. The energy of each pulse before and after the cell was recorded simultaneously using two pyrolectric joulemeters. This allows the energy absorbed, and hence the average number of photons absorbed per molecule, to be determined for each pulse. This is then averaged over a number of pulses. Full details are given by Gascooke et al.[10]

IRF decay traces at various bath gas pressures were recorded with a constant HFB pressure, typically 2.5 mTorr. This very low pressure was necessary to minimize blackbody radiation and to avoid any errors associated with large temperature rises within the cell. The low HFB pressures used also allow greater accuracy in the analysis of the data, which involves an extrapolation to infinite dilution in collider gas (see Results).

He (BOC), Ne (Spectra Gases), Ar (BOC), Kr (Spectra Gases), and Xe (Spectra Gases) were used directly as supplied. C_6F_6 (Aldrich, 99.9%) was degassed using several freeze−pump−thaw cycles prior to use.

Results

While IRMPA is an extremely useful method for preparing an initial ensemble of highly excited molecules at variable initial internal energies, it leads to a range of initial energies since molecules within the sample can absorb an integer number of photons, ranging from zero upward. Problems arise because the distribution can be bimodal, resulting from a near thermal population of those molecules that did not absorb and a higher energy distribution of molecules that absorbed many photons.[20] As discussed previously,[10] in the case of HFB there are two experimental measurements of UV absorption spectra before and after IRMPA, suggesting that the distribution produced is not bimodal,[21,22] and this is likely to be true for the conditions of our experiments. The IRMPA-IRF data were analyzed assuming that all HFB molecules absorb. This leads to a particular value for the average number of photons absorbed, and hence average initial energy, that determines the slope of the $\langle\langle \Delta E \rangle\rangle$ versus internal energy curve. Confirmation of the validity of this assumption was obtained by comparing the energy dependence of $\langle\langle \Delta E \rangle\rangle$ obtained from the IRMPA-IRF experiments for Ar with that obtained from the IC-IRF experiments (see also Table 1).[10]

TABLE 1: Lennard-Jones Parameters and the Energy Dependence of the Average Energy Transferred per Collision, $\langle\langle \Delta E \rangle\rangle$

collider	σ (nm)	ϵ/k_B (K)	$10^{10}k_{LJ}$ ($cm^3\ s^{-1}$)	k_1[a]	$-\langle\langle \Delta E \rangle\rangle$[b] ($cm^{-1}$)
He	0.255	10.22	6.98	$(4.60 \pm 0.14) \times 10^{-3}$	69 ± 2
Ne	0.282	32.0	3.92	$(6.42 \pm 0.17) \times 10^{-3}$	96 ± 3
Ar	0.347	113.5	4.15	$(8.16 \pm 0.36) \times 10^{-3}$	122 ± 5
Ar (UV)[c]				$(8.20 \pm 0.60) \times 10^{-3}$	126 ± 9
Kr	0.366	178	3.60	$(5.92 \pm 0.15) \times 10^{-3}$	88 ± 3
Xe	0.405	230	3.59	$(5.44 \pm 0.12) \times 10^{-3}$	82 ± 1
HFB	0.619	323	5.21		

[a] Evaluated from fits to the linear form, $-\langle\langle \Delta E \rangle\rangle = k_1\langle\langle E \rangle\rangle$. [b] Evaluated at 15 000 cm^{-1}. [c] IC-IRF experiments.[10]

From measurements of the laser fluence before, Φ_{in}, and after, Φ_{out}, the cell (with corrections for attenuation from cell windows), the average energy absorbed, $\langle\langle Q \rangle\rangle$, can be calculated via the relationship[20]

$$\langle\langle Q \rangle\rangle = \frac{\Phi_{in}}{NL} \ln\left(\frac{\Phi_{in}}{\Phi_{out}}\right) \quad (1)$$

where N is the concentration of the molecule of interest in the cell, and L is the cell length. This equation is valid for a collimated laser beam and absorption <10%.[20] When all molecules are excited, as assumed in this study (see above), then $\langle\langle Q \rangle\rangle$ is equal to $\langle\langle E \rangle\rangle$ at time zero. The fluences used in this work yield average initial energies of ~16 000 ± 1500 cm^{-1}.

Variation of Internal Energy with Time. The experiments measure IRF intensity as a function of time. IRF traces typical of those observed in the IRMPA experiments are shown in Figure 1. The usual methods for extracting the variation of the internal energy with time from these data have been described by Barker and co-workers.[2,23] They involve extrapolating the experimental intensity versus time decay curves to time zero where the initial energy is known. In recent data treatments, the IRF decay curves were converted from a time scale to a collision scale, and the fitted parameters in the intensity versus collisions expression were extrapolated to the limit of excited molecule infinitely dilute in collider gas.[23] The changes in IRF intensity with time (or number of collisions) can then be associated with changes in internal energy with time (or collision number) using calculated calibration curves.

We have chosen a different approach that involves fitting the internal energy versus time behavior directly to the

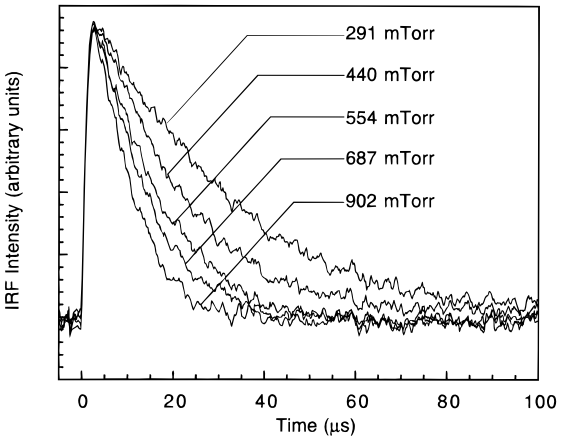

Figure 1. Infrared fluorescence decay curves for excited HFB prepared by IRMPA in the presence of the indicated pressures of Xe collider gas. $P_{HFB} = 2.5$ mTorr.

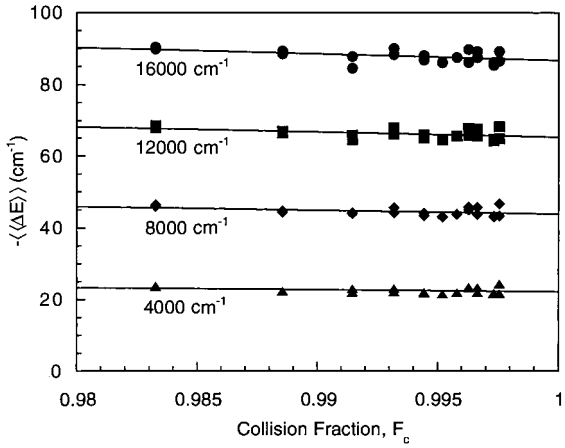

Figure 2. Average energy transferred per collision as a function of collision fraction for Xe collider gas.

experimental data. Full details are given elsewhere,[10] but a brief outline is presented here. The internal energy is assumed to follow the general functional form

$$E(t) = E_0 \exp[-k_{t_1}(t - t_0) - k_{t_2}(t - t_0)^2] \qquad (2)$$

where E_0 is the initial excitation energy and k_{t_1}, k_{t_2}, and t_0 are variable parameters in the fitting procedure. t_0 is an adjustable parameter necessary for the automated fitting procedure to overlay the experimental and fitted decay traces. In practice, the fitted value of t_0 is identical for each data set. This functional form was chosen because an exponential is the most widely used form for modeling energy decay, and through the presence of a second term (in t^2), the expression additionally allows for the roll-off in the average energy transferred per collision as reported by previous workers.[2,13]

An initial set of k_{t_1}, k_{t_2}, and t_0 parameters is used to generate an $E(t)$ function, as per eq 2. This $E(t)$ function is converted to an IRF intensity versus time function, IRF(t), using the theoretical expression relating the IRF intensity to the bulk average energy.[2,24] The applicability of the theoretical relationship has been extensively tested, and no occurrences have been found where the relationship has failed to hold.[2,23] An IRF intensity versus time curve, IR(t), is generated from the combination of IRF(t) and a function BBR(t), used to describe blackbody radiation.[25] This is necessary because, in general, the IRF signal contains components from both IRF and blackbody radiation (present due to the generation of heat during the collisional relaxation process). Thus, the experimental decays consist of a superposition of an IRF decay curve and a blackbody radiation rise. The calculated IR(t) is convoluted with the detector response function, SRF(t), determined experimentally, to yield the calculated function $I(t)$. $I(t)$ is compared with the experimental decay curve, the parameters k_{t_1}, k_{t_2}, t_0, and A_{BBR} are adjusted, and the process is repeated until the calculated and experimental traces converge; the entire process is automated. The Levenberg−Marquardt method of nonlinear least-squares fitting[26] was used to match an $E(t)$ function to an observed IR emission trace.

Extraction of Average Energy Transferred per Collision as a Function of Internal Energy. The IRF decay curves are measured over a range of HFB dilutions in the collider gas. For each curve, i.e., each dilution, values of k_{t_1}, k_{t_2}, and t_0 are determined as described above, giving an $E(t)$ function. This expression for $E(t)$ is converted to one for $E(Z)$, where Z, the collision number, is determined from t using the Lennard-Jones collision frequency.[27] The form of $E(Z)$ thus obtained is analytic (since $E(t)$ is analytic), and an expression is readily derived for $dE(Z)/dZ$, the bulk average energy transferred per collision, $\langle\langle \Delta E \rangle\rangle$. Thus, from eq 2

$$\langle\langle \Delta E \rangle\rangle = -\langle\langle E \rangle\rangle [k_{Z_1}{}^2 - 4k_{Z_2} \ln(\langle\langle E \rangle\rangle / E_0)]^{1/2} \qquad (3)$$

where k_{Z_1} and k_{Z_2} are related to k_{t_1} and k_{t_2} via the transformation from time to collision number. The bulk average energy is the average over the population distribution, and as the energy distribution evolves with time, only $\langle\langle \Delta E \rangle\rangle$, which is the bulk first moment, can be obtained directly from the evolution of the average energy.[2] These $\langle\langle \Delta E \rangle\rangle$ functions refer to particular mixtures of HFB and collider gas and thus include both HFB−HFB collisions and HFB−collider collisions. To extract the HFB−collider value alone, these $\langle\langle \Delta E \rangle\rangle$ functions must be extrapolated to infinite dilution of HFB in the collider gas. This is done by plotting $\langle\langle \Delta E \rangle\rangle$ as a function of the collision fraction, F_c, for a series of internal energy values, as shown in Figure 2 for Xe collider gas. The collision fraction is given by[2]

$$F_c = \frac{k_{LJ}^c N_c}{k_{LJ}^c N_c + k_{LJ}^p N_p} \qquad (4)$$

where k_{LJ}^c and k_{LJ}^p are the Lennard-Jones collision frequencies of the collider and parent gases respectively, and N_c and N_p are the number densities of collider and parent molecules, respectively. By extrapolating each $\langle\langle \Delta E \rangle\rangle$ versus F_c plot to $F_c = 1$, a $\langle\langle \Delta E \rangle\rangle$ value corresponding solely to HFB−collider energy transfer is obtained at each energy, $\langle\langle E \rangle\rangle$. This gives a set of points that is fit to the following functional form to obtain the final energy dependence of $\langle\langle \Delta E \rangle\rangle$:

$$\langle\langle \Delta E \rangle\rangle = \langle\langle E \rangle\rangle [k_1{}^2 - 4k_2 \ln(\langle\langle E \rangle\rangle / E_0)]^{1/2} \qquad (5)$$

The energy range for the applicability of eq 5 is from the initial average energy down to 5000 cm^{-1}. The values for $\langle\langle \Delta E \rangle\rangle$ obtained from the data analysis are included in Table 1. The uncertainties are the standard errors resulting largely from the extrapolation in the collision fraction plot (Figure 2). For all collision partners the parameters reveal $\langle\langle \Delta E \rangle\rangle$ to be essentially linear with energy (see Figure 3). The magnitude of the nonlinear term compared with the linear term, illustrated through a comparison of the ratios of these two terms when the average energy has fallen to half its initial value, is typically a few percent. Thus, for small values of k_2, eq 5 reduces to $\langle\langle \Delta E \rangle\rangle =$

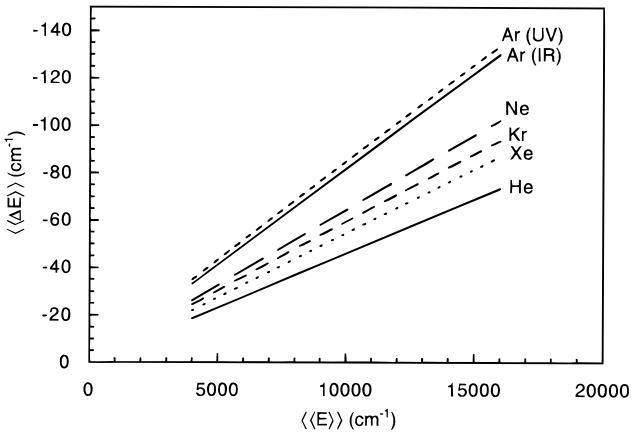

Figure 3. Average energy transferred per collision as a function of average internal energy; results for Ar (UV) are from ref 10.

TABLE 2: Average Energy Transferred per Collision, $-\langle\langle\Delta E\rangle\rangle$ (cm^{-1}), for the Deactivation of HFB by Noble Gases

	$-\langle\langle\Delta E\rangle\rangle$ for $\langle\langle E\rangle\rangle$ (cm^{-1}) =				excitation	
collider	51 800[a]	40 300[b]	24 000	15 000	method	ref
He	300	~286[c]	~162[c]	~57[c]	UV−193 nm	13
			110	69	IRMPA	this work
			200		theory-QCT[d]	16
Ne			154	96	IRMPA	this work
Ar	196	153	91	61	UV−193 nm	12
	540	~476[c]	~333[c]	~190[c]	UV−193 nm	13
		327	198	126	UV−248 nm	10
			194	122	IRMPA	this work
			149		theory-QCT[d]	16
Kr			139	88	IRMPA	this work
Xe			130	82	IRMPA	this work
			85		theory-QCT[d]	16

[a] Photon energy at 193 nm. [b] Photon energy at 248 nm. [c] Estimated from Figure 9 of Damm et al.[13] [d] Quasiclassical trajectory calculations.

$-k_1\langle\langle E\rangle\rangle$. The k_1 values found by fitting to this linear form for the colliders used in this study are shown in Table 1. Also shown in Table 1 are the values for the Lennard-Jones parameters and k_{LJ}. The parameters for He, Ar, and HFB were taken from Damm et al.,[13] and those for Ne, Kr, and Xe were taken from Mourits and Rummens.[28] The values for k_{LJ} were calculated using the empirical equation of Neufeld at al.[29] for the collision integral.

Discussion

Since we have obtained a functional form for $\langle\langle\Delta E\rangle\rangle$ from our data, we can compare our values of $\langle\langle\Delta E\rangle\rangle$ with those measured in previous studies, which have used initial excitation at 193[12,13] and 248 nm. All results for HFB with noble gas colliders are shown in Table 2. In a recent comparative study of HFB with Ar collider gas using both IC-IRF and IRMPA-IRF techniques, we demonstrated the viability of the IRMPA-IRF technique.[10] Previous experimental studies[12,13] of HFB collisional energy transfer based on the IC-UVA technique reported results for two of the noble gases, He and Ar. Allowing for extrapolation of the different studies to different energy regimes, comparison of our results with those of Damm et al.[13] shows reasonable agreement for He, but the agreement is not as good for Ar. The results obtained by Ichimura et al.[12] for Ar are somewhat lower, but their results were assessed by Damm et al.[13] as being obsolete because of the use of a UVA calibration curve obtained with an insufficient database. Our results for a full series of five noble gas colliders facilitate the establishment of a trend within the series. The average energy transferred per collision for these colliders was found to increase from He through to Ar; however, it subsequently decreased from Ar through to Xe.

The maximum $\langle\langle\Delta E\rangle\rangle$ observed for Ar collider suggests that there is a preferred deactivator mass in the noble gas series. It is worth noting that the trend observed in our study is very similar to that observed by Tardy,[30] who used the technique of IRMPA coupled with time-resolved optoacoustics to investigate the deactivation of C_6F_{14} and C_8F_{18} by the same series of five noble gases as used in our work. Tardy found that the relative collision efficiency (the deactivation rate constant relative to the hard-sphere collision rate constant) increased from He to Ne to Ar and then decreased to Kr followed by a slight leveling off for Xe. While the absolute values of this relative collision efficiency may have uncertainties, the observed trends for a series of similar colliders with a given excited species should be reliable for comparative purposes. Tardy carried out a satisfactory analysis of his results in terms of the simple billiard ball model (impulsive collision) by treating the excited polyatomic as a pseudodiatomic molecule and using the equation presented by Benson.[31]

Lenzer et al.[16,17] have carried out quasiclassical trajectory calculations on the deactivation of excited HFB (and benzene) by some mono- and polyatomic colliders, including the noble gases He, Ar, and Xe. The calculations were carried out for initial energies of 14 000, 24 000, 34 000, 40 700, and 53 270 cm^{-1}, but the authors used their results at 24 000 cm^{-1} for detailed comparisons between input parameters in the calculations and between calculations and experimental results. Their calculations for HFB at 24 000 cm^{-1} are shown in Table 2. As pointed out by Lenzer at al.,[16,17] the agreement between their trajectory calculations and experiment is excellent for benzene but less satisfying when compared with the experimental results of Damm et al.[13] for HFB. While the trajectory calculations for the magnitudes of $\langle\langle\Delta E\rangle\rangle$ are in reasonable agreement with our experiments for Ar collider, they are somewhat higher than experiment for He and lower than experiment for Xe. Also, the trend predicted by the trajectory calculations is a continuous decrease in the average energy transferred per collision from He to Ar to Xe, in contrast to our experiments which show a maximum for Ar in the noble gas series. Lenzer and Luther[17] suggest that inadequacies in the trajectory calculations for HFB are probably due to an insufficient representation of the intermolecular potential between F and Ar atoms.

There is considerable debate concerning the variation in the average energy transferred per collision with internal energy. Figure 3 shows the linear energy dependence of $\langle\langle\Delta E\rangle\rangle$ for each monatomic over the energy range studied. This is consistent with trends observed in earlier work based on IC-IRF and IC-UVA studies when extrapolated to low energies.[4,12,13] Also, despite the differences in absolute values of $\langle\langle\Delta E\rangle\rangle$ between trajectory calculations and experiment, the energy dependence of $\langle\langle\Delta E\rangle\rangle$ predicted by the trajectory calculations is essentially linear.[16,17]

The results obtained here for HFB may be compared with data on aromatics of similar size (e.g., benzene, toluene, pyrazine).[2,23] For convenience of qualitative comparison, the values for $\langle\langle\Delta E\rangle\rangle$ at 24 000 cm^{-1} are shown in Table 3, but the relativities are essentially the same at 15 000 cm^{-1}. The collisional deactivation of HFB shows much higher $\langle\langle\Delta E\rangle\rangle$

TABLE 3: Average Energy Transferred Per Collision, $-\langle\langle\Delta E\rangle\rangle$ (cm^{-1}), for Deactivation of Excited Aromatics by Noble Gases

excited molecule	$-\langle\langle\Delta E\rangle\rangle$ at $\langle\langle E\rangle\rangle = 24\,000$ cm^{-1} for collider					
	He	Ne	Ar	Kr	Xe	ref
HFB	~162		~333			13
			91			12
			198			10
	110	154	194	139	130	this work
benzene	23	20	30	34	36	2
toluene	62	77	112	110	124	2
pyrazine	22	33	32	51	52	23

values (between 3 and 10 times larger) when compared to these aromatics. The large difference in the energy dependence and absolute values of $\langle\langle\Delta E\rangle\rangle$ between HFB and toluene deactivated by Ar has been highlighted by Damm et al.[13] This much more efficient collisional deactivation of HFB has been suggested by Damm et al.[13] as probably due to the increased number of low-frequency modes. The increased efficiency of collisional energy transfer of HFB relative to these other aromatics is also supported by the trajectory calculations (at least for HFB versus benzene)[16,17] despite the differences in absolute values of $\langle\langle\Delta E\rangle\rangle$ between theory and experiment. The trajectory calculations show that the lower the vibrational frequencies the more efficient is the collisional energy transfer, as was suggested by Damm et al.[13]

Conclusions

The collisional deactivation of highly excited HFB by the series of noble gas colliders He, Ne, Ar, Kr, and Xe was studied using the IRMPA-IRF technique. The magnitude of the average energy transferred per collision was found to increase from He through to Ar; however, it subsequently decreased from Ar through to Xe. The average energy transferred per collision is a linear function of energy. For the same colliders, the $\langle\langle\Delta E\rangle\rangle$ values for HFB are much greater than those for the closely related aromatics, benzene, toluene, and pyrazine.

Acknowledgment. This work was supported by the Australian Research Council. The authors are grateful for the technical support provided by the staff of the University of Adelaide Chemical Engineering Department Workshop and the Flinders University Department of Physical Sciences Electronic Workshop. J.R.G. is grateful for the award of a Ferry Scholarship.

References and Notes

(1) Oref, I.; Tardy, D. C. *Chem. Rev.* **1990**, *90*, 1407.

(2) Barker, J. R.; Toselli, B. M. *Int. Rev. Phys. Chem.* **1993**, *12*, 305. Barker, J. R.; Brenner, J. D.; Toselli, B. M. In *Vibrational Energy Transfer Involving Large and Small Molecules;* Advances in Chemical Kinetics and Dynamics; Barker, J. R., Ed.; JAI Press: Greenwich, CT, 1995.

(3) Hartland, G. V.; Qin, D.; Dai, H.-L.; Chen, C. *J. Chem. Phys.* **1997**, *107*, 2890.

(4) Barker, J. R.; Yerram, M. L. In *Multiphoton Processes*; Smith, S. J.; Knight, P. L., Eds.; Cambridge University Press: London, 1988.

(5) Brown, T. C.; King, K. D.; Zellweger, J.-M.; Barker, J. R. *Ber. Bunsen-Ges. Phys. Chem.* **1985**, *89*, 301. Zellweger, J.-M.; Brown, T. C.; Barker, J. R. *J. Chem. Phys.* **1985**, *83*, 6251. Zellweger, J.-M.; Brown, T. C.; Barker, J. R. *J. Chem. Phys.* **1985**, *83*, 6261. Zellweger, J.-M.; Brown, T. C.; Barker, J. R. *J. Phys. Chem.* **1986**, *90*, 461.

(6) Abel, B.; Hippler, H.; Troe, J. *J. Chem. Phys.* **1992**, *96*, 8863. Abel, B.; Hippler, H.; Troe, J. *J. Chem. Phys.* **1992**, *96*, 8872.

(7) Coronado, E. A.; Ferrero, J. C. *J. Phys. Chem. A* **1997**, *101*, 9603.

(8) Coronado, E. A.; Rinaldi, C. A.; Velardez, G. F.; Ferrero, J. C. *Chem. Phys. Lett.* **1994**, *227*, 164.

(9) Coronado, E. A.; Ferrero, J. C. *Chem. Phys. Lett.* **1996**, *257*, 674.

(10) Gascooke, J. R.; Alwahabi, Z. T.; King, K. D.; Lawrance, W. D. *J. Chem. Phys.*, to be published.

(11) Rinaldi, C. A.; Ferrero, J. C.; Vázquez, M. A.; Azcárate, M. L.; Quel, E. J. *J. Chem. Phys.* **1996**, *100*, 9745.

(12) Ichimura, T.; Mori, Y.; Nakashima, N.; Yoshihara, K. *Chem. Phys. Lett.* **1984**, *104*, 533. Ichimura, T.; Mori, Y.; Nakashima, N.; Yoshihara, K. *J. Chem. Phys.* **1985**, *83*, 117. Ichimura, T.; Takahashi, M.; Mori, Y. *Chem. Phys. Lett.* **1984**, *114*, 111.

(13) Damm, M.; Hippler, H.; Olschewski, H. A.; Troe, J.; Willner, J. *Z. Phys. Chem.* (*Munich*) **1990**, *166*, 129.

(14) Phillips, D. *J. Chem. Phys.* **1967**, *46*, 5679.

(15) Watanabe, A.; Koga, Y.; Sugawara, K.; Takeo, H.; Fukuda, K.; Matsumura, C.; Keehn, P. M. *Spectrochim. Acta* **1990**, *46A*, 463.

(16) Lenzer, T.; Luther, K.; Troe, J.; Gilbert, R. G.; Lim, K. F. *J. Chem. Phys.* **1995**, *103*, 626.

(17) Lenzer, T.; Luther, K. *Ber. Bunsen-Ges. Phys. Chem.* **1997**, *101*, 581.

(18) Eaton, V. J.; Steele, D. *J. Mol. Spectrosc.* **1973**, *48*, 446. Pearce, R. U. R.; Steele, D.; Radklife, K. *J. Mol. Struct.* **1973**, *15*, 409.

(19) Poel, K. L.; Alwahabi, Z. T.; King, K. D. *Chem. Phys.* **1995**, *201*, 263. Poel, K. L.; Alwahabi, Z. T.; King, K. D. *J. Chem. Phys.* **1996**, *105*, 1420. Poel, K. L.; Glavan, C. M.; Alwahabi, Z. T.; King, K. D. *J. Phys. Chem. A* **1997**, *101*, 5614.

(20) Bagratashvili, V. N.; Letokhov, V. S.; Makarov, A. A.; Ryabov, E. A. *Multiple Photon Infrared Laser Photophysics and Photochemistry*; Harwood: London, 1985.

(21) Speiser, S.; Grunwald, E. *Chem. Phys. Lett.* **1980**, *73*, 438.

(22) Chen, X.; Li, L.; Sun, F.; Zhang, C. *Acta Opt. Sin.* **1984,** *4*, 781.

(23) Miller, L. A.; Barker, J. R. *J. Chem. Phys.* **1996**, *105*, 1383. Miller, L. A.; Cook, C. D.; Barker, J. R. *J. Chem. Phys.* **1996**, *105*, 3012.

(24) Durana, J. F.; McDonald, J. D. *J. Chem. Phys.* **1977**, *64*, 2518.

(25) Atkins, P. W. *Physical Chemistry*, 5th ed.; Oxford University Press: Oxford, 1992.

(26) Marquardt, D. W. *J. Soc. Indust. Appl. Math.* **1963**, *11*, 431. Press, W. H.; Teukolsky, S. A.; Vetterling, W. T.; Flannery, B. P. *Numerical Recipes in Fortran*; Cambridge University Press: Cambridge, 1992.

(27) Hippler, H.; Troe, J.; Wendelken, H. J. *J. Chem. Phys.* **1983**, *78*, 6709.

(28) Mourits, F. M.; Rummens, H. A. *Can. J. Chem.* **1977**, *55*, 3007.

(29) Neufeld, P. D.; Janzen, A. R.; Aziz, R. A. *J. Chem. Phys.* **1972**, *57*, 1100.

(30) Tardy, D. C. *J. Chem. Phys.* **1993**, *99*, 963.

(31) Benson, S. W. *The Foundations of Chemical Kinetics*; Krieger Publishing: Florida, 1982.